

## Janus graphene: A two-dimensional half-auxetic carbon allotrope with a nonchemical Janus configuration

Linfeng Yu <sup>1</sup>, Jianhua Xu,<sup>1</sup> Chen Shen <sup>2</sup>, Hongbin Zhang,<sup>2</sup> Xiong Zheng,<sup>1</sup> Huimin Wang <sup>3</sup>,  
Zhenzhen Qin <sup>4</sup> and Guangzhao Qin <sup>1,5,\*</sup>

<sup>1</sup>State Key Laboratory of Advanced Design and Manufacturing Technology for Vehicle, College of Mechanical and Vehicle Engineering, Hunan University, Changsha 410082, People's Republic of China

<sup>2</sup>Institute of Materials Science, Technical University of Darmstadt, Darmstadt 64287, Germany

<sup>3</sup>Hunan Key Laboratory for Micro-Nano Energy Materials and Device and School of Physics and Optoelectronics, Xiangtan University, Xiangtan 411105, Hunan, China

<sup>4</sup>School of Physics and Microelectronics, Zhengzhou University, Zhengzhou 450001, China

<sup>5</sup>Greater Bay Area Institute for Innovation, Hunan University, Guangzhou 511300, Guangdong Province, People's Republic of China



(Received 17 July 2023; revised 23 December 2023; accepted 22 January 2024; published 11 March 2024)

We propose a nonchemical intrinsic Janus configuration and identify it in a pure  $sp^2$  hybridized carbon monolayer, termed Janus graphene. The spontaneous unilateral growth of carbon atoms drives the nonchemical Janus configuration in Janus graphene, which is totally different from the chemical effect in common Janus materials such as MoSSe. A structure-independent half-auxetic behavior is mapped in Janus graphene, that the structure maintains expansion whether stretched or compressed, which lies in the key role of the  $p_z$  orbital. With the unique half-auxeticity that emerged in the nonchemical Janus configuration, Janus graphene enriches the functional carbon family as a promising candidate for micro/nanoelectronic device applications.

DOI: [10.1103/PhysRevB.109.L121402](https://doi.org/10.1103/PhysRevB.109.L121402)

**Introduction.** The carbon element has an extremely strong bonding ability and abundant bonding forms in chemical reactions, such as linear alkyne ( $sp$ ), planar olefin ( $sp^2$ ), and tetrahedral alkane ( $sp^3$ ) bonds. The superior performance of graphene, such as superconducting [1–3] and quantum Hall effect [4,5], motivate researchers to extend their interest from three-dimensional to two-dimensional (2D) carbon crystals. For example, experimental preparations have been conducted for monolayer amorphous carbon [6], biphenylene [7], and monolayer fullerene [8]. Furthermore, the initial prediction of bulk T-carbon was made in 2011 [9], followed by its experimental synthesis in 2017 [10]. The synthesis and discovery of these promising carbon configurations has encouraged the designing and screening of multifunctional carbon monolayers with specific technological interests.

As an emerging class of nanomaterials, Janus nanostructures are functional structures with different properties composed of two materials (or different elements) on the same object, driven by chemical effects. “Janus bead” was first proposed by the French scientist Casagrande in 1989 to describe the unique structure of semihydrophobic and semihydrophilic materials on the surface of spherical particles [11]. Then, in 1991, the name “Janus” of the two-faced god in Greek mythology was first proposed by the French physicist Gennes to describe particles with dual properties in his Nobel Prize speech [12]. Subsequently, Janus materials

have been widely used in many fields, such as biology, energy, chemistry, and physics, due to their unique asymmetry [13–21].

2D Janus atomic crystals are monolayer materials with structural symmetry breaking caused by chemical effects. Tremendous effort has been devoted to designing and synthesizing the 2D Janus material with chemisorption [22,23], atomic substitution [17], and stacked heterojunctions [24], facilitating the generation of many 2D nanomaterials with unique physical properties, such as MoSSe [17]. Note that the Janus properties of current Janus materials depend on chemical effects, i.e., different adatoms, functional groups, or elemental effects. Currently, the preparation of Janus materials relies on chemical interactions, including atomic substitution [17,25,26], chemisorption [22,23,27,28], and heterojunction [24,29,30], which divides Janus materials into three types as shown in Fig. S1 of the Supplemental Material [31]: (1) The element-type Janus structures, where different elements are arranged along the out-of-plane direction, such as 2H-MoSSe [17]; (2) the adatom-type Janus structures, which are formed by the adsorption of different atoms on both sides along the out-of-plane sides, such as graphenelike Janus materials [32]; (3) the heterojunction-type Janus structures, which are van der Waals layered compounds formed by different types of monolayers along out-of-plane directions, such as graphene/MgX ( $X=S, Se$ ), and graphene/BN [33–36]. However, intrinsic carbon materials, where only carbon atoms exist, can hardly achieve Janus properties without extrinsic chemical effects. Such a problem inspires us to design 2D Janus carbon materials with unique symmetry breaking using advanced crystal design methods.

\*Corresponding author: [gzqin@hnu.edu.cn](mailto:gzqin@hnu.edu.cn)

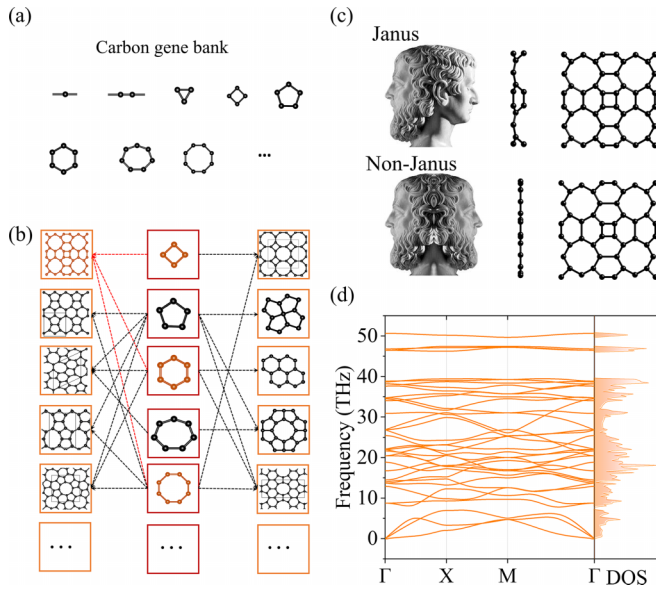


FIG. 1. Janus graphene and its evolution. (a) Two-dimensional carbon structure gene bank. (b) Two-dimensional carbon structure constructed by carbon gene recombination. (c) Comparison of Janus and non-Janus phases. (d) The phonon dispersion and phonon density of states (DOS) of Janus graphene.

This Letter proposes an intrinsic nonchemical Janus configuration in purely  $sp^2$  hybridized carbon monolayer, named as Janus graphene, which is totally different from the previously reported Janus structures driven by chemical effects. An emerging half-auxetic property is found in the pure  $sp^2$ -hybrid Janus graphene, which breaks the notion that pure  $sp^2$ -hybridized carbon monolayers cannot exhibit intrinsic negative Poisson's ratio (NPR) behavior. The successfully designed Janus graphene exhibits its unique Janus structural and unconventional half-auxeticity, which would be a strong candidate for the applications of carbon materials in micro/nano electronic devices.

**Carbon gene recombination.** Based on 2D carbon geometry features, the carbon gene recombination strategy can be proposed here to design 2D carbon with different configurations, which maps the geometric properties into quotient maps for recombination and screening of 2D carbon structures. Figure S2(a) demonstrates a schematic diagram of the structure identification process, and the initial idea of the strategy is to build a carbon gene bank according to the bonding characteristics of carbon materials. According to the number of atoms, 2D carbon genes can be divided into monoatomic chain, diatomic chain, triangular ring, tetragonal ring, pentagonal ring, hexagonal ring, etc., as shown in Fig. 1(a). In the  $xy$  plane, 2D carbon can be broken down into these carbon genes, and likewise, it can also be reconstituted to form other carbon monolayers. Among them, four hexagonal rings are reconstructed along the tetragonal rings, and then octagonal rings are introduced by periodic mirroring in the tetragonal lattice [Fig. S2(b)], forming a carbon monolayer with  $sp^2$  hybridization, i.e., Janus graphene, as shown in Figs. 1(b) and 1(c). Such evolution can also be used to reconstruct other 2D carbon configurations [37,38] with specific carbon genes

[Fig. 1(b)]. Phonon dispersion visualizes lattice vibrations in the Brillouin zone, reflecting the dynamic stability of Janus graphene due to all positive frequencies as shown in Fig. 1(d). More computational details as well as structural and stability insights can be found in Supplemental Notes S1, S2 and Figs. S1, S2, and S3 [31].

**Nonchemical Janus structure.** The primitive cell of the optimized structure contains 12 atoms with the space group of  $P4mm$  (99). Interestingly, this 2D carbon allotrope protrudes along one side of out of plane but exhibits planar features on the other side, which symbolizes the two-faced god Janus in ancient Roman mythology, hence the name "Janus graphene." In carbon material, graphene can be formed with the above-mentioned Janus carbon materials through asymmetric chemistry [22,23,27,28], but usually leads to some irreversible changes in physical and chemical properties, such as the destruction of the Dirac cone [22]. Unlike chemically driven Janus materials, the Janus configuration of Janus graphene is natural and intrinsic, as it purely consists of carbon atoms. Thus, it is considered as a undiscovered class of intrinsic Janus structure type. Unlike the Janus material summarized in Fig. S1, the intrinsic Janus structure relies on an uneven distribution of the structure in space, i.e., the carbon atoms break the plane symmetry through an inhomogeneous arrangement to form the Janus phase, which leads to bifunctionality on both sides in the out-of-plane direction.

**Emerging half-auxeticity.** The unique Janus configuration brings extraordinary structural evolution performance, especially the auxetic behavior. Diverse auxetic behaviors are found in Janus graphene compared to typical graphene and penta graphene. Graphene exhibits a total positive Poisson's ratio (Total-PPR) behavior [Fig. 2(a)] in that it contracts (stretches) in orthogonal directions when stretched (compressed), consistent with previous study [39]. Unlike graphene, a total negative Poisson's ratio (Total-NPR) behavior is found in penta graphene [Fig. 2(b)], i.e., it exhibits stretch (compression) behavior when stretched (compressed) in orthogonal directions [40]. Unusually, Janus graphene [Fig. 2(c)] always expands regardless of whether it is stretched or compressed, i.e., half-negative Poisson's ratio (Half-NPR) behavior. Schematic representations of diverse Poisson's ratio behaviors are further plotted in Figs. 2(d) and 2(e) to understand their differences, i.e., total-PPR, total-NPR, and half-NPR. The in-plane half-NPR behavior was first proposed by Ma *et al.*, but so far has only been found in borides [41,42]. The scarcity and magic of the half-NPR behavior in Janus graphene contrasts with its mono [Fig. 2(g)], binary [Fig. 2(h)], and ternary [Fig. 2(i)] counterparts. Unlike traditional auxetic behavior, that the material expands (shrinks) when stretched (compressed), half-auxetic behavior reveals a mechanical phenomenon whereby materials always expand, whether stretched or compressed. The current auxetic behavior is only found in the  $sp^3$  (or  $sp^2$ - $sp^3$ )-hybridized configuration in carbon materials [43]. We searched the 108 carbon structures included in the 2D carbon database [44] and the 1114  $sp^2$ -hybridized 2D carbon structures screened by Shi *et al.* [45], but found no auxetic behavior reported in the pure  $sp^2$ -hybridized carbon configuration. The reason lies in that the strong  $sp^2$  hybridization favors the graphenelike planar structure, which hinders the generation of the reentry

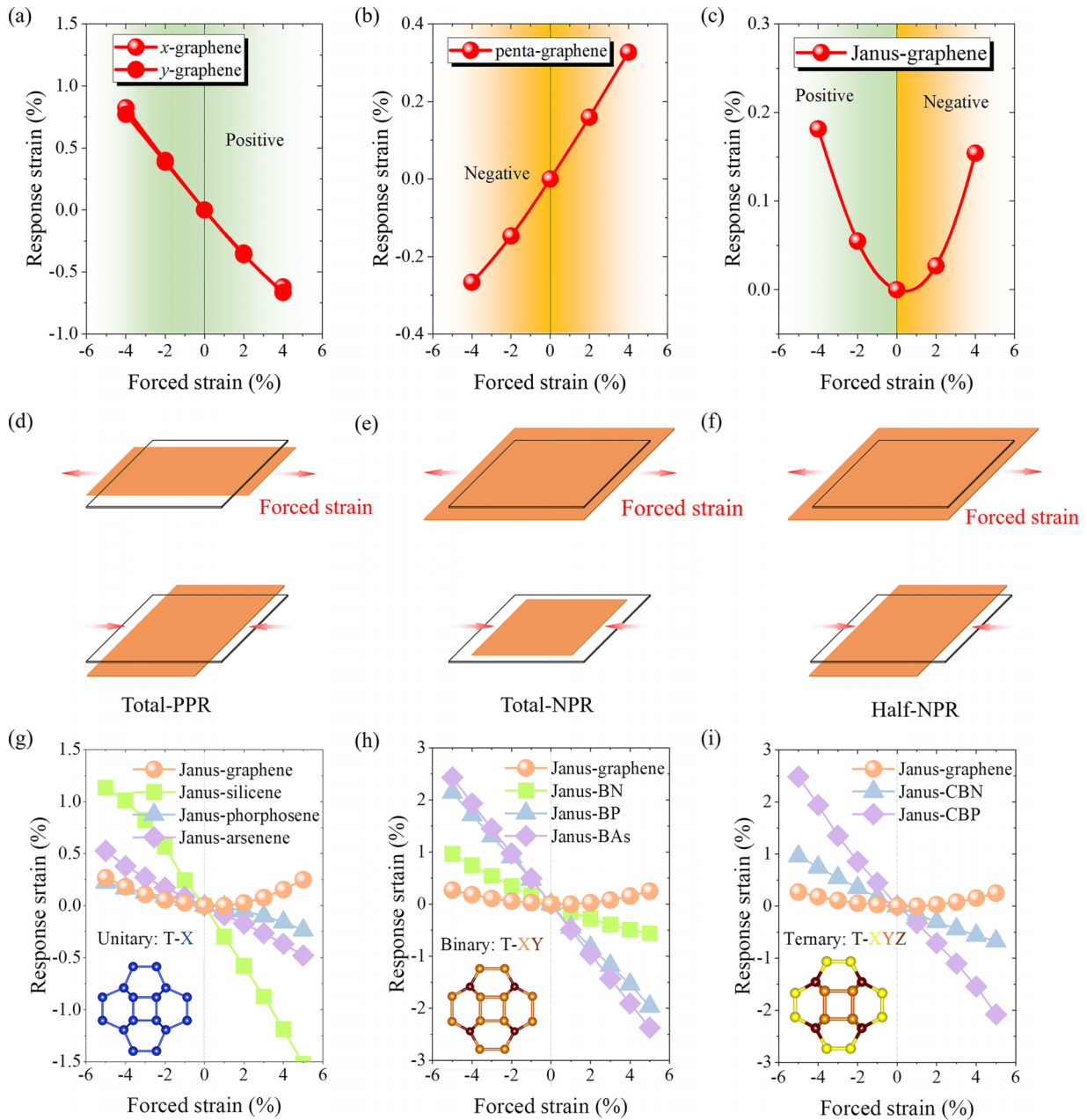


FIG. 2. Auxetic behavior of two-dimensional carbon. Strain curves and schematic diagrams representing different Poisson's ratio behaviors for (a) graphene with a (d) total positive Poisson's ratio (Total-PPR) behavior, (b) penta graphene with a (e) total negative Poisson's ratio (Total-NPR) behavior, and (c) Janus graphene with a (f) half-negative Poisson's ratio (Half-NPR) behavior. Comparison of Poisson's ratio behavior of Janus graphene with other two-dimensional Janus compounds, including (g) unary, (h) binary, and (i) ternary phases.

mechanism that induces NPR behavior. Here, the unique geometric evolution enables the NPR behavior to be extended to pure  $sp^2$ -hybridized carbon configurations, and this in-plane half-auxetic behavior is revealed in carbon materials. In addition, we also show the stress-strain curve diagram of Janus graphene under uniaxial strain in Fig. S4 in the Supplemental Material.

*The role of the  $p_z$  orbital.* Before closing, the electronic properties of Janus graphene are investigated to further understand the emerging features from the intrinsic Janus structure, as shown in Fig. 3. The precise HSE06 functional identifies a wide bandgap of 2.21 eV for Janus graphene, higher than the 1.16 eV of the Perdew-Burke-Ernzerhof functional as shown

in Fig. 3(a) and Supplemental Material Note S3. Compared with graphene, the valence-band maximum (VBM) and the conduction-band minimum (CBM) mainly contributed by the  $p_z$  orbital are not at the same high-symmetry point, where the  $p_z$  orbital plays a major role for bonded states (Supplemental Material Note S3 and Fig. S5). The three-dimensional images of VBM and CBM are further revealed by Fig. 3(b). In Janus graphene, the deviation of the out-of-plane  $\pi$  bonds in space in the vertical direction leads to the breaking of out-of-plane symmetry. In the planar phase, the intrinsic Poisson's ratio is generally positive because the electrons of the  $p_z$  orbitals are coupled in the large ring-shaped  $\pi$  bonds and cannot be easily activated by the force field to generate a reentrant mechanism

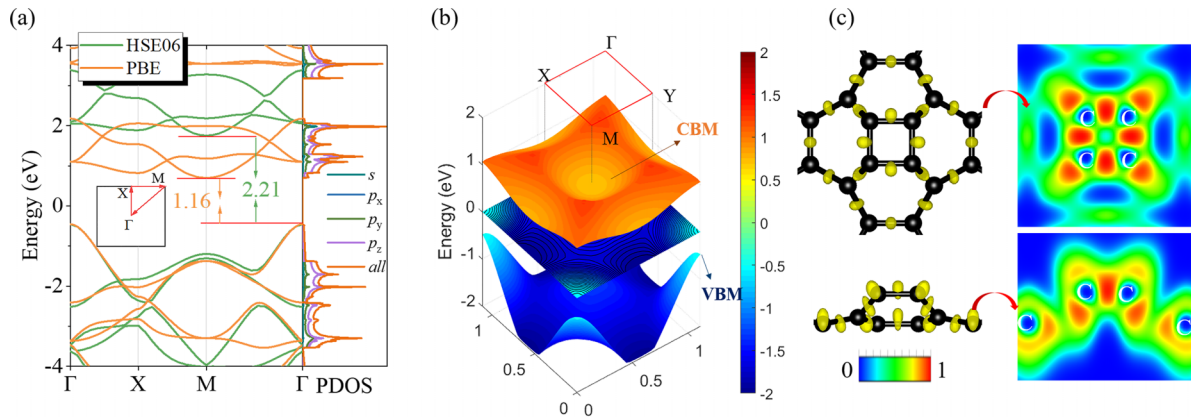


FIG. 3. Electronic properties of Janus graphene. (a) Electronic bandgap of Janus graphene. (b) Three-dimensional (3D) valence-band maximum (VBM) and the conduction-band minimum (CBM) in Janus graphene. (c) The 3D and 2D electron localization function (ELF) of Janus graphene.

due to the robust  $\pi$  bonds and symmetric planar structure. Typically, planar graphene often needs to apply a strain field of more than 15% to activate the reentry mechanism to achieve NPR [39,46], which is usually unacceptable in practical operations. As shown in Fig. 3(c), the covalent electrons in the C-C bond in Janus graphene are unevenly distributed along the out-of-plane direction, i.e., strong asymmetry. This leads to intrinsic Janus properties in the structure and makes the reentry mechanism easier to activate due to the more isolated  $p_z$  electrons. During the structure evolution, the  $p_z$  electrons in Janus graphene deviate from the planar state and become more sensitive to the external force field. Under a stretching force field, it is forced to couple in the in-plane direction, producing an anomalous response in geometrical angles ( $\beta$  response in Supplemental Material Note S4 and Figs. S6, S7 and S8), exciting potential reentry mechanisms, and finally leading to NPR. The unique orbital evolution of Janus graphene brings it nonchemical Janus properties and unconventional NPR effects in terms of geometric and mechanical responses, making it an excellent platform for studying structural and functional linkages.

**Conclusion.** In summary, we proposed an unprecedented nonchemical intrinsic Janus configuration concept, and engineered a pure  $sp^2$  hybridized 2D carbon allotrope with this configuration. This carbon allotrope exhibits double-faced features similar to the Roman god Janus, hence named as Janus graphene. Different from the traditional Janus configuration, the Janus configuration of Janus graphene does not depend on chemical effects, which is formed by the carbon

atoms growth towards the out-of-plane unilateral side of the 2D plane. The unique Janus geometry maps the unconventional half-auxetic property that the Janus graphene always expands whether it is stretched or compressed. This half-auxetic property shows a structure-independence feature. We extend this auxeticity to pure  $sp^2$ -hybridized configurations and identify its origin in the structure's diverse response to strain. The unique Janus structure and unconventional half-auxetic properties combined with wide-bandgap semiconducting properties endow Janus graphene with multifunction, providing a strong candidate for micro-nanoelectronic devices.

**Acknowledgments.** This work is supported by the National Natural Science Foundation of China (Grant No. 52006057), the Natural Science Foundation of Chongqing, China (Grant No. CSTB2022NSCQ-MSX0332), the Fundamental Research Funds for the Central Universities (Grant No. 531119200237), and the State Key Laboratory of Advanced Design and Manufacturing for Vehicle Body at Hunan University (Grant No. 52175013). H.W. is supported by the National Natural Science Foundation of China (Grant No. 51906097). Z.Q. is supported by the National Natural Science Foundation of China (Grants Nos.12274374 and No. 11904324) and the China Postdoctoral Science Foundation (2018M642776).

G.Q. supervised the project. L.Y. performed all the calculations, analysis, and writing. All the authors contributed to interpreting the results. The Letter was written by L.Y. with contributions from all the authors.

- [1] M. Yankowitz, S. Chen, H. Polshyn, Y. Zhang, K. Watanabe, T. Taniguchi, D. Graf, A. F. Young, and C. R. Dean, Tuning superconductivity in twisted bilayer graphene, *Science* **363**, 1059 (2019).
- [2] B. Uchoa and A. H. Castro Neto, Superconducting states of pure and doped graphene, *Phys. Rev. Lett.* **98**, 146801 (2007).
- [3] Y. Cao, V. Fatemi, S. Fang, K. Watanabe, T. Taniguchi, E. Kaxiras, and P. Jarillo-Herrero, Unconventional superconduc-

tivity in magic-angle graphene superlattices, *Nature (London)* **556**, 43 (2018).

- [4] K. S. Novoselov, Z. Jiang, Y. Zhang, S. V. Morozov, H. L. Stormer, U. Zeitler, J. C. Maan, G. S. Boebinger, P. Kim, and A. K. Geim, Room-temperature quantum Hall effect in graphene, *Science* **315**, 1379 (2007).
- [5] V. P. Gusynin and S. G. Sharapov, Unconventional integer quantum Hall effect in graphene, *Phys. Rev. Lett.* **95**, 146801 (2005).

- [6] C.-T. Toh, H. Zhang, J. Lin, A. S. Mayorov, Y.-P. Wang, C. M. Orofeo, D. B. Ferry, H. Andersen, N. Kakenov., Z. Guo *et al.*, Synthesis and properties of free-standing monolayer amorphous carbon, *Nature (London)* **577**, 199 (2020).
- [7] Q. Fan, L. Yan, M.-W. Tripp, O. Krejčí, S. Dimosthenous, S.-R. Kachel, M. Chen, A.-S. Foster, U. Koert, P. Liljeroth *et al.*, Biphenylene network: A nonbenzenoid carbon allotrope, *Science* **372**, 852 (2021).
- [8] L. Hou, X. Cui, B. Guan, S. Wang, R. Li, Y. Liu, D. Zhu, and J. Zheng, Synthesis of a monolayer fullerene network, *Nature (London)* **606**, 507 (2022).
- [9] X.-L. Sheng, Q.-B. Yan, F. Ye, Q.-R. Zheng, and G. Su, T-carbon: A novel carbon allotrope, *Phys. Rev. Lett.* **106**, 155703 (2011).
- [10] J. Zhang, R. Wang, X. Zhu, A. Pan, C. Han, X. Li, D. Zhao, C. Ma, W. Wang, H. Su, and C. Niu, Pseudo-topotactic conversion of carbon nanotubes to T-carbon nanowires under picosecond laser irradiation in methanol, *Nat. Commun.* **8**, 683 (2017).
- [11] C. Casagrande, P. Fabre, E. Raphaël, and M. Veyssié, “Janus Beads”: Realization and behaviour at water/oil interfaces, *Europhys. Lett.* **9**, 251 (1989).
- [12] P.-G. de Gennes, Soft matter (Nobel Lecture), *Angew. Chem. Int. Ed. Engl.* **31**, 842 (1992).
- [13] Y. Dudai and M. Carruthers, The Janus face of mnemosyne, *Nature (London)* **434**, 567 (2005).
- [14] S. B. Wilson and T. L. Delovitch, Janus-like role of regulatory iNKT cells in autoimmune disease and tumour immunity, *Nat. Rev. Immunol.* **3**, 211 (2003).
- [15] J. Yan, M. Bloom, S. C. Bae, E. Luijten, and S. Granick, Linking synchronization to self-assembly using magnetic Janus colloids, *Nature (London)* **491**, 578 (2012).
- [16] E. Poggi and J.-F. Gohy, Janus particles: From synthesis to application, *Colloid. Polym. Sci.* **295**, 2083 (2017).
- [17] A.-Y. Lu, H. Zhu, J. Xiao, C.-P. Chuu, Y. Han, M.-H. Chiu, C.-C. Cheng, C.-W. Yang, K.-H. Wei, Y. Yang *et al.*, Janus monolayers of transition metal dichalcogenides, *Nat. Nanotechnol.* **12**, 744 (2017).
- [18] H.-C. Yang, Y. Xie, J. Hou, A. K. Cheetham, V. Chen, and S. B. Darling, Janus membranes: Creating asymmetry for energy efficiency, *Adv. Mater.* **30**, 1801495 (2018).
- [19] K.-H. Roh, D. C. Martin, and J. Lahann, Biphasic Janus particles with nanoscale anisotropy, *Nat. Mater.* **4**, 759 (2005).
- [20] B. Wang, B. Li, B. Zhao, and C. Y. Li, Amphiphilic Janus gold nanoparticles via combining “solid-state Grafting-to” and “grafting-from” methods, *J. Am. Chem. Soc.* **130**, 11594 (2008).
- [21] N. Santschi and R. Gilmour, A Janus cyclohexane ring, *Nat. Chem.* **7**, 467 (2015).
- [22] L. Zhang, J. Yu, M. Yang, Q. Xie, H. Peng, and Z. Liu, Janus graphene from asymmetric two-dimensional chemistry, *Nat. Commun.* **4**, 1443 (2013).
- [23] H. Wu, W. Yi, Z. Chen, H. Wang, and Q. Du, Janus graphene oxide nanosheets prepared via Pickering emulsion template, *Carbon* **93**, 473 (2015).
- [24] L. Ju, M. Bie, X. Zhang, X. Chen, and L. Kou, Two-dimensional Janus van der Waals heterojunctions: A review of recent research progresses, *Front. Phys.* **16**, 13201 (2020).
- [25] A. B. Maghirang, Z.-Q. Huang, R. A. B. Villaos, C.-H. Hsu, L.-Y. Feng, E. Florido, H. Lin, A. Bansil, and F.-C. Chuang, Predicting two-dimensional topological phases in Janus materials by substitutional doping in transition metal dichalcogenide monolayers, *npj 2D Mater. Appl.* **3**, 35 (2019).
- [26] S.-D. Guo, W.-Q. Mu, J.-H. Wang, Y.-X. Yang, B. Wang, and Y.-S. Ang, Strain effects on the topological and valley properties of the Janus monolayer VSiGeN<sub>4</sub>, *Phys. Rev. B* **106**, 064416 (2022).
- [27] J. Sun, M. Sadd, P. Edenborg, H. Grönbeck, P. H. Thiesen, Z. Xia, V. Quintano, R. Qiu, A. Matic, and V. Palermo, Real-time imaging of Na<sup>+</sup> reversible intercalation in “Janus” graphene stacks for battery applications, *Sci. Adv.* **7**, eabf0812 (2021).
- [28] L. Wang, Q. Wen, P. Jia, M. Jia, D. Lu, X. Sun, L. Jiang, and W. Guo, Light-driven active proton transport through photoacid- and photobase-doped Janus graphene oxide membranes, *Adv. Mater.* **31**, 1903029 (2019).
- [29] P. Wang, Y.-X. Zong, H.-Y. Wen, J.-B. Xia, and Z.-M. Wei, Electronic properties of two-dimensional Janus atomic crystal, *Acta Phys. Sin.* **70**, 026801 (2021).
- [30] S. Arra, R. Babar, and M. Kabir, van der Waals heterostructure for photocatalysis: Graphitic carbon nitride and Janus transition-metal dichalcogenides, *Phys. Rev. Mater.* **3**, 095402 (2019).
- [31] See Supplemental Material at <http://link.aps.org/supplemental/10.1103/PhysRevB.109.L121402> for more details. The Supplemental Material also contains Refs. [47–50].
- [32] S.-W. Ng, N. Noor, and Z. Zheng, Graphene-based two-dimensional Janus materials, *NPG Asia Mater.* **10**, 217 (2018).
- [33] M. M. Furchi, F. Höller, L. Dobusch, D. K. Polyushkin, S. Schuler, and T. Mueller, Device physics of van der Waals heterojunction solar cells, *npj 2D Mater. Appl.* **2**, 3 (2018).
- [34] M. M. Furchi, A. Pospischil, F. Libisch, J. Burgdörfer, and T. Mueller, Photovoltaic effect in an electrically tunable van der Waals heterojunction, *Nano Lett.* **14**, 4785 (2014).
- [35] D. Rhodes, S. H. Chae, R. Ribeiro-Palau, and J. Hone, Disorder in van der Waals heterostructures of 2D materials, *Nat. Mater.* **18**, 541 (2019).
- [36] A. K. Geim and I. V. Grigorieva, Van der Waals heterostructures, *Nature* **499**, 419 (2013).
- [37] U. Choudhry, S. Yue, and B. Liao, Origins of significant reduction of lattice thermal conductivity in graphene allotropes, *Phys. Rev. B* **100**, 165401 (2019).
- [38] H. Yin, X. Shi, C. He, M. Martinez-Canales, J. Li, C. J. Pickard, C. Tang, T. Ouyang, C. Zhang, and J. Zhong, Stone-Wales graphene: A two-dimensional carbon semimetal with magic stability, *Phys. Rev. B* **99**, 041405(R) (2019).
- [39] G. Qin and Z. Qin, Negative Poisson’s ratio in two-dimensional honeycomb structures, *npj Comput. Mater.* **6**, 51 (2020).
- [40] S. Zhang, J. Zhou, Q. Wang, X. Chen, Y. Kawazoe, and P. Jena, Penta-graphene: A new carbon allotrope, *Proc. Natl. Acad. Sci. USA* **112**, 2372 (2015).
- [41] Z. Gao, Q. Wang, W. Wu, Z. Tian, Y. Liu, F. Ma, Y. Jiao, and S. A. Yang, Monolayer RhB<sub>4</sub>: Half-auxeticity and almost ideal spin-orbit Dirac point semimetal, *Phys. Rev. B* **104**, 245423 (2021).
- [42] F. Ma, Y. Jiao, W. Wu, Y. Liu, S. A. Yang, and T. Heine, Half-auxeticity and anisotropic transport in Pd decorated two-dimensional boron sheets, *Nano Lett.* **21**, 2356 (2021).
- [43] L. Yu, Z. Qin, H. Wang, X. Zheng, and G. Qin, Half-negative Poisson’s ratio in graphene+ with intrinsic Dirac nodal loop, *Cell Rep. Phys. Sci.* **3**, 100790 (2022).
- [44] 2D Carbon Database, <http://www.c2d.site/>

- [45] X. Shi, S. Li, J. Li, T. Ouyang, C. Zhang, C. Tang, C. He, and J. Zhong, High-throughput screening of two-dimensional planar  $sp^2$  carbon space associated with a labeled quotient graph, *J. Phys. Chem. Lett.* **12**, 11511 (2021).
- [46] Z. Qin, G. Qin, and M. Hu, Origin of anisotropic negative Poisson's ratio in graphene, *Nanoscale* **10**, 10365 (2018).
- [47] J. P. Perdew, K. Burke, and M. Ernzerhof, Generalized gradient approximation made dimple, *Phys. Rev. Lett.* **77**, 3865 (1996).
- [48] G. Kresse and J. Hafner, *Ab initio* molecular-dynamics simulation of the liquid-metal–amorphous-semiconductor transition in germanium, *Phys. Rev. B* **49**, 14251 (1994).
- [49] H. J. Monkhorst and J. D. Pack, Special points for Brillouin-zone integrations, *Phys. Rev. B* **13**, 5188 (1976).
- [50] L. Chaput, A. Togo, I. Tanaka, and G. Hug, Phonon-phonon interactions in transition metals, *Phys. Rev. B* **84**, 094302 (2011).